Mechanism for the partial synchronization in three coupled chaotic systems

Woochang Lim and Sang-Yoon Kim
Department of Physics, Kangwon National University, Chunchon, Kangwon-Do 200-701, Korea
(Received 2 September 2004; revised manuscript received 21 December 2004; published 24 March 2005)

We investigate the dynamical mechanism for the partial synchronization in three coupled one-dimensional maps. A completely synchronized attractor on the diagonal becomes transversely unstable via a blowout bifurcation, and then a two-cluster state, exhibiting on-off intermittency, appears on an invariant plane. If the newly created two-cluster state is transversely stable, then partial synchronization occurs on the invariant plane; otherwise, complete desynchronization takes place. It is found that the transverse stability of the intermittent two-cluster state may be determined through the competition between its laminar and bursting components. When the laminar (bursting) component is dominant, partial synchronization (complete desynchronization) occurs through the blowout bifurcation. This mechanism for the occurrence of partial synchronization is also confirmed in three coupled multidimensional invertible systems, such as coupled Hénon maps and coupled pendula.

DOI: 10.1103/PhysRevE.71.036221 PACS number(s): 05.45.Xt

I. INTRODUCTION

Recently, synchronization of coupled chaotic systems has attracted much attention because of its potential practical applications (e.g., see Ref. [1]). For a sufficiently strong coupling, complete synchronization of chaotic systems occurs (i.e., all subsystems become synchronized) [2–5]. However, as the coupling parameter decreases and passes a threshold value, the fully synchronized attractor on the invariant synchronization subspace becomes transversely unstable via a blowout bifurcation [6–10]. Then, partial synchronization, where some of the subsystems synchronize while others do not, or complete desynchronization may occur for three or more coupled systems [11–16]. In particular, partial synchronization (or clustering) has been extensively investigated in globally coupled systems where each subsystem is coupled to all the other subsystems with equal strength [17–19].

Here, we are interested in whether the asynchronous attractor created via a supercritical blowout bifurcation of the fully synchronized attractor is partially synchronized or completely desynchronized. Examples of both partially synchronized attractors [11,13–15] and completely desynchronized attractors [12,16] were reported. These previous results show that occurrence of partial synchronization depends on the type of base map constituting the coupled system and the type of coupling between the base maps. However, the underlying mechanism for the occurrence of partial synchronization remains unclear.

This paper is organized as follows. As a simple model where partial synchronization may occur, we consider three coupled one-dimensional (1D) maps with a parameter $p(0 \leqslant p \leqslant 1/3)$ tuning the degree of asymmetry in the coupling from unidirectional coupling ($p=0$) to symmetric coupling ($p=1/3$). This model can be used to represent the three-cluster dynamics in an ensemble of N globally coupled 1D maps and the parameter p describes the distribution of the elements between the three clusters. For both extreme cases of the unidirectional and symmetric couplings, partial synchronization [11] and complete desynchronization [16] occur, respectively. In Sec. II A, we investigate the dynamical mechanism for the occurrence of partial synchronization by increasing the parameter p from 0 to 1/3. An asynchronous two-cluster state appears on an invariant plane via a supercritical blowout bifurcation of the fully synchronized attractor on the diagonal. A typical trajectory in the newly created two-cluster state exhibits on-off intermittency [20–28], where long episodes of laminar (i.e., nearly synchronous) evolution near the diagonal are occasionally interrupted by short-term bursts. When the asymmetry parameter p is less than a threshold value p^* (i.e., $0 \leqslant p < p^*$), the two-cluster state on the invariant plane is transversely stable, and hence partial synchronization occurs. However, for $p > p^*$ a completely desynchronized attractor, occupying a three-dimensional (3D) finite volume, appears, because the two-cluster state is transversely unstable. It is found that such a transverse stability of the intermittent two-cluster state may be determined via competition between its laminar and bursting components. When the "transverse strength" of the laminar component is larger (smaller) than that of the bursting component, the two-cluster state becomes transversely stable (unstable), and hence a partially synchronized (completely desynchronized) attractor appears through the supercritical blowout bifurcation. These results are also confirmed in Sec. II B for the case of three coupled multidimensional invertible period-doubling systems such as coupled Hénon maps and coupled pendula. Hence, the mechanism for the occurrence of partial synchronization seems to be of wide significance because it holds in typical three-coupled period-doubling systems. However, note that the transverse stability of a two-cluster state for the three-coupled case does not imply transverse stability in the N globally coupled case. As was shown in [18], chaotic two-cluster states created via blowout bifurcations are transversely unstable in an ensemble of N globally coupled 1D maps. (A detailed explanation of distinction between the two types of transverse stability for the three-coupled and N globally coupled cases is also given in the last part of Sec. II A.) Finally, we give a summary in Sec. III.

II. DYNAMICAL MECHANISM FOR THE OCCURRENCE OF PARTIAL SYNCHRONIZATION

A. Partial synchronization in three coupled 1D maps

We investigate the dynamical mechanism for the occurrence of partial synchronization in three coupled 1D maps with a parameter tuning the asymmetry in the coupling.

$$x_{t+1}^{(i)} = f(x_t^{(i)}) + \varepsilon\left(\sum_{j=1}^{3} p_j f(x_t^{(j)}) - f(x_t^{(i)})\right), \quad i = 1,2,3, \quad (1)$$

where $x_t^{(i)}$ is a state variable of the ith element at a discrete time t, the uncoupled dynamics ($\varepsilon=0$) is governed by the 1D map $f(x)=1-ax^2$ with a control parameter a, ε is a coupling parameter, and p_j denotes the coupling weight for the jth element ($\Sigma_{j=1}^{3} p_j = 1$). Here, the asymmetric coupling naturally appears when studying the three-cluster dynamics in an ensemble of N globally coupled 1D maps [17–19], where each 1D map is coupled to all the other ones with equal strength,

$$x_{t+1}^{(i)} = f(x_t^{(i)}) + \varepsilon\left(\frac{1}{N}\sum_{j=1}^{N} f(x_t^{(j)}) - f(x_t^{(i)})\right). \quad (2)$$

For the case of three clusters with N_j elements in each jth cluster ($j=1,2,3$), Eq. (2) is reduced to the three-coupled system of Eq. (1), where $p_j(=N_j/N)$ represents the fraction of the total population of elements in the jth cluster. Two extreme cases of the unidirectional and symmetric couplings were previously considered. The unidirectionally coupled map with $p_2=p_3=0$ (i.e., $p_1=1$), where the first drive subsystem with the state variable $x^{(1)}$ acts on the second and third response subsystems with the state variables $x^{(2)}$ and $x^{(3)}$, was studied in [11], and partial synchronization was observed to occur on an invariant plane via a supercritical blowout bifurcation of the fully synchronized attractor on the diagonal. On the other hand, a completely desynchronized 3D attractor appears through the supercritical blowout bifurcation for the case of symmetric coupling with $p_1=p_2=p_3=1/3$ [16]. To connect these two extreme cases, we consider a path with $p_2=p_3\equiv p(0\leqslant p\leqslant 1/3)$ in the p_2-p_3 plane, and then the parameter p tunes the degree of asymmetry in the coupling of Eq. (1) from the unidirectional coupling ($p=0$) to the symmetric coupling ($p=1/3$).

From now on, we investigate the dynamical origin for the occurrence of partial synchronization by varying the asymmetry parameter p in the three coupled 1D maps of Eq. (1) for $a=1.95$. We first consider complete synchronization occurring in the case of strong coupling. Such complete synchronization is independent of p. Figures 1(a) and 1(b) show a fully synchronized attractor on the invariant diagonal for $\varepsilon=0.5$. The longitudinal stability of a synchronized trajectory $\{x_t^*(=x_t^{(1)}=x_t^{(2)}=x_t^{(3)})\}$ on the attractor against the perturbation along the diagonal is determined by its longitudinal Lyapunov exponent

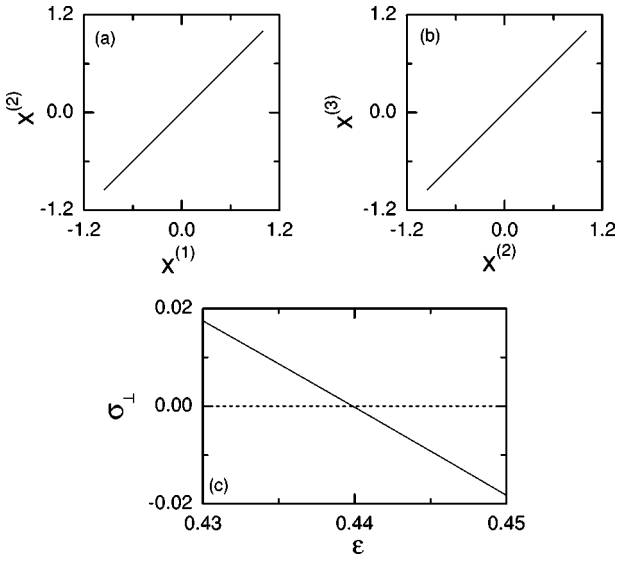

FIG. 1. Projections of a fully synchronized attractor onto the (a) $x^{(1)}$-$x^{(2)}$ and (b) $x^{(2)}$-$x^{(3)}$ planes for $a=1.95$ and $\varepsilon=0.5$. (c) Plot of $\sigma_\perp$ (transverse Lyapunov exponent of the fully synchronized attractor) versus ε for $a=1.95$. The data of $\sigma_\perp$ are represented by a solid line.

$$\sigma_\parallel = \lim_{M\to\infty}\frac{1}{M}\sum_{t=0}^{M-1} \ln|f'(x_t^*)|, \quad (3)$$

where the prime represents the differentiation of f with respect to x. This longitudinal Lyapunov exponent is just the Lyapunov exponent of the 1D map f. For $a=1.95$, we have $\sigma_\parallel=0.5795$, and hence the attractor is a chaotic one. On the other hand, the transverse stability of the fully synchronized attractor against perturbation across the diagonal (i.e., asynchronous perturbation) is determined by its transverse Lyapunov exponent with a twofold multiplicity,

$$\sigma_\perp = \sigma_\parallel + \ln|1-\varepsilon|. \quad (4)$$

A plot of $\sigma_\perp$ versus ε is shown in Fig. 1(c). If ε is relatively large such that $\sigma_\parallel < -\ln|1-\varepsilon|$, then the transverse Lyapunov exponent $\sigma_\perp$ is negative, and hence the fully synchronized attractor becomes transversely stable. However, as ε decreases and passes a threshold value ε^* (=0.4398), the fully synchronized attractor becomes transversely unstable, because the transverse Lyapunov exponent $\sigma_\perp$ becomes positive. Then, an asynchronous attractor, containing the diagonal, is created via a supercritical blowout bifurcation, but its type depends on the value of p.

In the unidirectionally coupled case with $p=0$, a partially synchronized attractor appears via a supercritical blowout bifurcation on the invariant $\Pi_{23}[=\{(x^{(1)},x^{(2)},x^{(3)})|x^{(2)}=x^{(3)}\}]$ plane, as shown in Figs. 2(a) and 2(b) for $\varepsilon=0.42$. The partially synchronized attractor is a chaotic one with two longitudinal Lyapunov exponents $\sigma_{\parallel,1}$ (=0.5795) and $\sigma_{\parallel,2}$ (=−0.014)], and it is transversely stable against the perturbation across the Π_{23} plane, because its transverse Lyapunov exponent $\sigma_\perp$ (=−0.014) is negative. On the other hand, for the symmetrically coupled case with $p=1/3$, a completely

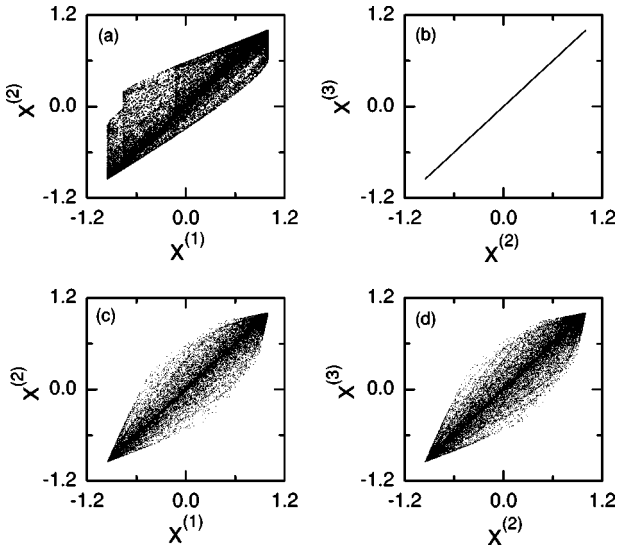

FIG. 2. Projections of the partially synchronized attractor onto the (a) $x^{(1)}$-$x^{(2)}$ and (b) $x^{(2)}$-$x^{(3)}$ planes for $a=1.95$ and $\varepsilon=0.42$ in the unidirectionally coupled case with $p=0$. Projections of the completely desynchronized attractor onto the (c) $x^{(1)}$-$x^{(2)}$ and (d) $x^{(2)}$-$x^{(3)}$ planes for $a=1.95$ and $\varepsilon=0.42$ in the symmetrically coupled case with $p=1/3$.

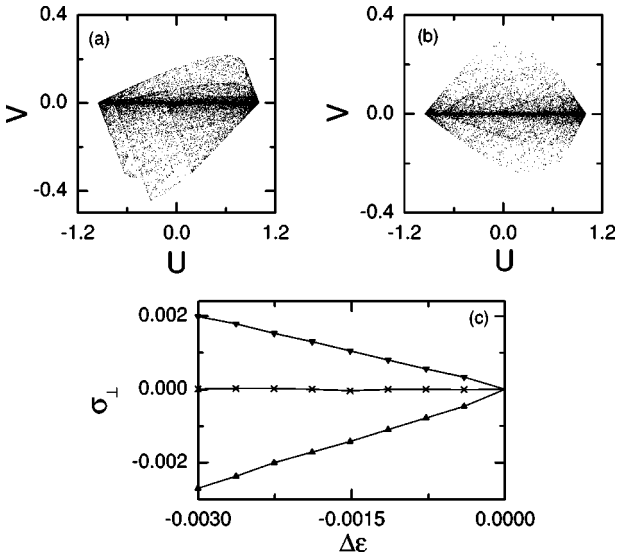

FIG. 3. (a) Transversely stable ($\sigma_\perp=-0.0027$) two-cluster state for $p=0$ and (b) transversely unstable ($\sigma_\perp=0.002$) two-cluster for $p=1/3$ in the U-V plane when $a=1.95$ and $\Delta\varepsilon[=\varepsilon-\varepsilon^*(=0.4398)]=-0.003$. (c) Plot of $\sigma_\perp$ (transverse Lyapunov exponent of the two-cluster state) versus $\Delta\varepsilon$ for $a=1.95$ [$p=0$ (up triangles), 0.146 (crosses), 1.3 (down triangles)]. Straight lines between the data symbols are plotted only to guide the eye.

desynchronized attractor, occupying a finite 3D volume, appears through a supercritical blowout bifurcation, as shown in Figs. 2(c) and 2(d) for $\varepsilon=0.42$, and it is a hyperchaotic attractor with three positive Lyapunov exponents ($\sigma_1=0.539$, $\sigma_2=0.021$, and $\sigma_3=0.01$). Such complete desynchronization occurs because the two-cluster state on the Π_{23} plane, created via the supercritical blowout bifurcation, becomes transversely unstable, as will be shown below.

When the fully synchronized attractor on the diagonal becomes transversely unstable, a two-cluster state appears on the invariant Π_{23} plane through a supercritical blowout bifurcation. This two-cluster state satisfies $x_t^{(1)}\equiv X_t$ and $x_t^{(2)}=x_t^{(3)}\equiv Y_t$, and its dynamics is governed by a reduced 2D map,

$$X_{t+1}=f(X_t)+2p\varepsilon[f(Y_t)-f(X_t)], \tag{5a}$$

$$Y_{t+1}=f(Y_t)+(1-2p)\varepsilon[f(X_t)-f(Y_t)]. \tag{5b}$$

For the accuracy of numerical calculations [29], we introduce new coordinates U and V,

$$U=\frac{X+Y}{2},\quad V=\frac{X-Y}{2}. \tag{6}$$

Then the invariant diagonal is transformed into a new invariant line $V=0$. In these new coordinates, the 2D reduced map of Eq. (5) becomes

$$U_t=1-a(U_t^2+V_t^2)-2a\varepsilon(1-4p)U_tV_t, \tag{7a}$$

$$V_t=2a(\varepsilon-1)U_tV_t. \tag{7b}$$

Figures 3(a) and 3(b) show the two-cluster states, created via supercritical blowout bifurcations, in the U-V plane for the unidirectionally ($p=0$) and symmetrically ($p=1/3$) coupled cases, respectively. These two-cluster states are chaotic attractors in the reduced 2D map (i.e., they are chaotic attractors in the restricted Π_{23} plane). However, their transverse stability against perturbation across the invariant Π_{23} plane depends on the value of p. Only when the two-cluster state is transversely stable, it becomes an attractor in the whole 3D space. To determine the transverse stability of a two-cluster state, we numerically follow a typical trajectory in the two-cluster state until its length L becomes 10^8, and then the transverse Lyapunov exponent for the trajectory segment with length L is given by

$$\sigma_\perp=\frac{1}{L}\sum_{t=0}^{L-1}\ln|(1-\varepsilon)f'(U_t-V_t)|. \tag{8}$$

A plot of $\sigma_\perp$ versus $\Delta\varepsilon$ ($=\varepsilon-\varepsilon^*$) is given in Fig. 3(c) [$p=0$ (up triangles), 0.146 (crosses), and $1/3$ (down triangles)], where $\varepsilon^*(=0.4398)$ is the blowout bifurcation point of the fully synchronized attractor. For the case of unidirectional coupling ($p=0$), the two-cluster state is transversely stable, because its transverse Lyapunov exponent $\sigma_\perp$ is negative, and hence partial synchronization occurs on the Π_{23} plane via a supercritical blowout bifurcation (i.e., a partially synchronized attractor appears on the Π_{23} plane). On the other hand, as p is increased from 0, the value of $\sigma_\perp$ increases; eventually it becomes zero for a threshold value p^* ($\simeq 0.146$), and then it becomes positive. Hence, for $p^*<p\leqslant 1/3$, complete desynchronization takes place through a supercritical blowout bifurcation (i.e., a completely desynchronized 3D attractor appears), because the two-cluster on the Π_{23} plane becomes transversely unstable. Examples in Figs. 3(a) and 3(b) for $\Delta\varepsilon=-0.003$ show the transversely stable

($\sigma_\perp = -0.0027$) and unstable ($\sigma_\perp = 0.002$) two-cluster states for $p=0$ and $1/3$, respectively.

We now investigate the mechanism for the transition from partial synchronization to complete desynchronization by varying the asymmetry parameter p. A typical trajectory in the two-cluster state, born via a supercritical blowout bifurcation, exhibits on-off intermittency near the main diagonal. We use a small quantity d^* for the threshold value of the magnitude of the transverse variable $d(=|V|)$ such that for $d < d^*$ the trajectory is considered to be in the laminar (off) state, where it exhibits a nearly synchronous motion, while for $d > d^*$ it is considered in the bursting (on) state. Thus, a typical trajectory may be decomposed into laminar and bursting components. Then, dynamical properties of the two-cluster state may be understood through competition of the laminar and bursting components [10]. Here, we are concerned about the transverse stability of an intermittent two-cluster state. Its transverse Lyapunov exponent $\sigma_\perp$ [see Eq. (8) for the transverse Lyapunov exponent of a trajectory segment] can be given by the sum of the two weighted transverse Lyapunov exponents of the laminar and bursting components, $\Sigma_\perp^l$ and $\Sigma_\perp^b$:

$$\sigma_\perp = \Sigma_\perp^l + \Sigma_\perp^b \tag{9a}$$

$$= \Sigma_\perp^b - |\Sigma_\perp^l|, \tag{9b}$$

where the laminar component always has a negative weighted transverse Lyapunov exponent ($\Sigma_\perp^l < 0$). For each component ($i=l,b$), the weighted transverse Lyapunov exponent $\Sigma_\perp^i$ is given by the product of the fraction μ_i of time spent in the i state and its transverse Lyapunov exponent $\sigma_\perp^i$, i.e.,

$$\Sigma_\perp^i = \mu_i \sigma_\perp^i, \quad \mu_i = \frac{L_i}{L},$$

$$\sigma_\perp^i = \frac{1}{L_i} {\sum_{t \in i \text{ state}}}' \ln|(1-\varepsilon) f'(U_t - V_t)| \quad (i = l,b), \tag{10}$$

where L_i is the time spent in the i state for a trajectory segment of length L and the primed summation is performed in each i state. Then, the sign of $\sigma_\perp$ may be determined through competition between the laminar and bursting components [see Eq. (9b)]. When the "transverse strength" of the laminar component [i.e., the magnitude of the weighted transverse Lyapunov exponent ($|\Sigma_\perp^l|$)] is larger (smaller) than that of the bursting component (i.e., $\Sigma_\perp^b$), partial synchronization (complete desynchronization) occurs, because the two-cluster becomes transversely stable (unstable).

Figures 4(a)–4(f) show the fraction $\mu_{l(b)}$ of the laminar (bursting) time [i.e., the time spent in the laminar (bursting) state], the transverse Lyapunov exponent $\sigma_\perp^{l(b)}$ of the laminar (bursting) component, and the weighted transverse Lyapunov exponent $\Sigma_\perp^{l(b)}$ of the laminar (bursting) component when the threshold value for the laminar state is $d^* = 10^{-4}$ [30]. For the case of the laminar component, both μ_l and $\sigma_\perp^l$ are nearly independent of p, and hence its weighted transverse Lyapunov exponent $\Sigma_\perp^l (= \mu_l \sigma_\perp^l)$ becomes nearly the same,

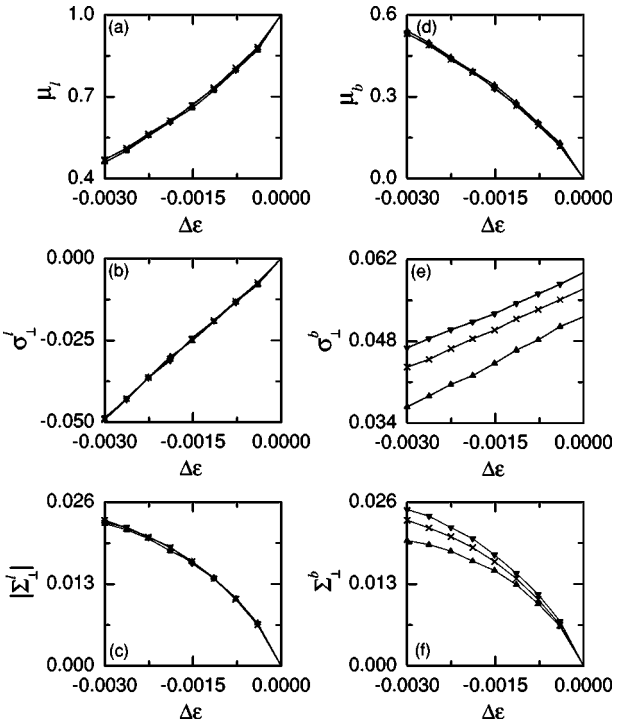

FIG. 4. Plots of (a) [(d)] the fraction $\mu_{l(b)}$ of the laminar (bursting) time, (b) [(e)] the transverse Lyapunov exponent $\sigma_\perp^{l(b)}$ of the laminar (bursting) component, and (c) [(f)] the weighted transverse Lyapunov exponents $\Sigma_\perp^{l(b)}$ of the laminar (bursting) component versus $\Delta\varepsilon[=\varepsilon-\varepsilon^*(=0.4398)]$ for $a=1.95$ with $p=0$ (up triangles), 0.146 (crosses), and $1/3$ (down crosses). Straight lines between the data symbols are plotted only to guide the eye.

irrespective of p [see Figs. 4(a)–4(c)]. On the other hand, the transverse Lyapunov exponent $\sigma_\perp^b$ of the bursting component increases as p is increased from zero [see Fig. 4(e); $p=0$ (up triangles), 0.146 (crosses), and $1/3$ (down triangles)], although its fraction $\mu_b[=1-\mu_l]$ of the bursting time is nearly independent of p, as shown in Fig. 4(d). Hence, the transverse strength of the bursting component [i.e., $\Sigma_\perp^b (= \mu_b \sigma_\perp^b)$] becomes larger as p is increased from zero [see Fig. 4(f)]. For $p=0$ (up triangles), the laminar component is dominant, because $|\Sigma_\perp^l| > \Sigma_\perp^b$. Hence, the two-cluster becomes transversely stable, and it becomes an attractor in the whole 3D phase space (i.e., partial synchronization occurs). However, as p is increased from zero, $\Sigma_\perp^b$ increases, while $|\Sigma_\perp^l|$ is nearly independent of p. Eventually, for a threshold value p^* [$\simeq 0.146$ (crosses)], the transverse strength of the bursting and laminar components becomes balanced (i.e., $\Sigma_\perp^b = |\Sigma_\perp^l|$), and then the bursting component becomes dominant for $p^* < p \leqslant 1/3$ [e.g., see the case of $p=1/3$ (down triangles)], because $\Sigma_\perp^b > |\Sigma_\perp^l|$. Thus, when passing the threshold value p^*, a transition from partial synchronization to complete desynchronization occurs. Consequently, for $0 \leqslant p < p^*$, there exists a partially synchronized attractor with $\sigma_\perp < 0$ on the invariant Π_{23} plane [e.g., see Figs. 2(a) and 2(b) for $p=0$], while for $p^* < p \leqslant 1/3$, a completely desynchronized 3D attractor appears [e.g., see Figs. 2(c) and 2(d) for $p=1/3$] because the two-cluster on the Π_{23} plane is transversely unstable.

The above transition from a partially synchronized to a completely desynchronized attractor could be understood as follows. The newly created intermittent two-cluster on the invariant Π_{23} plane includes an infinite number of asynchronous unstable periodic orbits that are off the invariant diagonal. Some of these unstable periodic orbits are transversely stable, while some others are transversely unstable. It is conjectured that as p is increased from zero, the strength of the group of asynchronous unstable periodic orbits with positive transverse Lyapunov exponents might increase, which may result in the observed increase in $\sigma_\perp^b$.

To sum up the main results of this section, we consider an intermittent two-cluster state created via a blowout bifurcation in the three-coupled 1D maps of Eq. (1) and show that the sign of its transverse Lyapunov exponent $\sigma_\perp$ of Eq. (8) can be determined through competition between the laminar and bursting components. However, we note that the transverse stability of a two-cluster state in the three-coupled 1D maps does not imply its transverse stability in an ensemble of N globally coupled 1D maps of Eq. (2). In fact, it was shown in [18] that two-cluster states created via blowout bifurcations in the N globally coupled 1D maps are transversely unstable for all the cases of distributions of elements between the two clusters. To make the point clear, we consider a two-cluster state $(x_t^{(1)}=\cdots=x_t^{(N_1)}\equiv X_t, x_t^{(N_1+1)}=\cdots=x_t^{(N)}\equiv Y_t)$ with N_i elements in the ith cluster ($i=1, 2$). Then, there exist two transverse Lyapunov exponents determining the transverse stability of the two-cluster state

$$\sigma_{\perp,1}=\lim_{L\to\infty}\frac{1}{L}\sum_{t=0}^{L-1}\ln|(1-\varepsilon)f'(X_t)|,$$

$$\sigma_{\perp,2}=\lim_{L\to\infty}\frac{1}{L}\sum_{t=0}^{L-1}\ln|(1-\varepsilon)f'(Y_t)|. \tag{11}$$

Here, $\sigma_{\perp,1}$ and $\sigma_{\perp,2}$ with N_1-1 and N_2-1 multiplicities determine the stability against perturbations destroying the synchronization of the first and second clusters, respectively. As shown in Fig. 6 of Ref. [18], the first largest transverse Lyapunov exponent $\sigma_{\perp,1}$ is positive for all values of the distribution parameter q $(=N_2/N)$, and hence all two-cluster states (created via blowout bifurcations) become transversely unstable. Following the similar procedure developed in the above three-coupled case [see Eq. (9b)], the transverse instability of all two-cluster states is also determined through competition between their laminar and bursting components. Since its bursting component is dominant for all q, any two-cluster state (created through a blowout bifurcation) becomes transversely unstable for the N globally coupled case. This is in contrast to our three-coupled case, where only one transverse Lyapunov exponent $\sigma_\perp$ of Eq. (8) determines the transverse stability of the two-cluster state $(x_t^{(1)}=X_t, x_t^{(2)}=x_t^{(3)}=Y_t)$ on the Π_{23} plane. We note that the transverse Lyapunov exponent $\sigma_\perp$, determining stability against perturbation breaking the synchrony of the second cluster $(x_t^{(2)}=x_t^{(3)})$, corresponds to the second transverse Lyapunov exponent $\sigma_{\perp,2}$ in Eq. (11) for the N globally coupled case. [However, for the three-coupled case, there is no transverse Lyapunov exponent corresponding to $\sigma_{\perp,1}$ in Eq. (11), because there exists only one element $x_t^{(1)}$ in the first cluster.] Thus, in our three-coupled case partial synchronization (complete desynchronization) is found to occur via a blowout bifurcation when the laminar (bursting) component is dominant. Finally, we emphasize that our method to determine the transverse stability of an intermittent two-cluster state through its decomposition into the laminar and bursting components may be applied to a large class of coupled systems (including the three-coupled and globally coupled cases we consider).

B. Partial synchronization in three-coupled multidimensional invertible systems

The results obtained in the preceding section are of wide significance, because the 1D map is a representative model for a large class of period-doubling systems. As examples, we study coupled multidimensional invertible systems, exhibiting period doublings, and find similar results.

First, we consider three coupled Hénon maps:

$$x_{t+1}^{(i)}=f(x_t^{(i)})-y_t^{(i)}+\varepsilon[M_t-f(x_t^{(i)})],\quad y_{t+1}^{(i)}=bx_t^{(i)}, \tag{12a}$$

$$M_t\equiv(1-2p)f(x_t^{(1)})+pf(x_t^{(2)})+pf(x_t^{(3)}), \tag{12b}$$

where $(x_t^{(i)},y_t^{(i)})$ $(i=1, 2, 3)$ is a state vector of the ith subsystem at a discrete time t, $f(x)=1-ax^2$, ε is a coupling parameter, $p(0\leqslant p\leqslant 1/3)$ is a parameter tuning the degree of asymmetry in the coupling from the unidirectional $(p=0)$ to symmetric coupling $(p=1/3)$, M_t can be regarded as a "weighted" mean field, and $b(|b|<1)$ is a damping parameter. As in the case of three coupled 1D maps, the three coupled Hénon maps may also be used as a model system for investigating the three-cluster dynamics in an ensemble of globally coupled Hénon maps.

Here, we fix the values of b and a at $b=0.1$ and $a=1.83$ and investigate the mechanism for the occurrence of partial synchronization by varying the asymmetry parameter p. For a sufficiently strong coupling, there exists a completely synchronized attractor $[x_t^{(1)}=x_t^{(2)}=x_t^{(3)}, y_t^{(1)}=y_t^{(2)}=y_t^{(3)}]$, independently of p. When the coupling parameter ε decreases and passes a threshold value $\varepsilon^*(=0.3574)$, the completely synchronized attractor becomes transversely unstable, because its largest transverse Lyapunov exponent becomes positive. Then, a new asynchronous two-cluster state, exhibiting on-off intermittency, is born on an invariant subspace $\{(x^{(1)},y^{(1)},x^{(2)},y^{(2)},x^{(3)},y^{(3)})|x^{(2)}=x^{(3)},y^{(2)}=y^{(3)}\}$ via a supercritical blowout bifurcation. If this two-cluster is transversely stable against the perturbation across the invariant subspace, it becomes a partially synchronized attractor in the whole phase space; otherwise, a completely desynchronized attractor, occupying a finite 6D volume, appears. The dynamics of this two-cluster, satisfying $x_t^{(1)}\equiv X_t^{(1)}$, $y_t^{(1)}\equiv Y_t^{(1)}$, $x_t^{(2)}=x_t^{(3)}\equiv X_t^{(2)}$, and $y_t^{(2)}=y_t^{(3)}\equiv Y_t^{(2)}$, is governed by a reduced 4D map,

$$X_{t+1}^{(1)}=f(X_t^{(1)})-Y_t^{(1)}+2p\varepsilon[f(X_t^{(2)})-f(X_t^{(1)})], \tag{13a}$$

$$Y_{t+1}^{(1)}=bX_t^{(1)}, \tag{13b}$$

$$X_{t+1}^{(2)} = f(X_t^{(2)}) - Y_t^{(2)} + (1-2p)\varepsilon[f(X_t^{(1)}) - f(X_t^{(2)})], \tag{13c}$$

$$Y_{t+1}^{(2)} = bX_t^{(2)}. \tag{13d}$$

As in the coupled 1D maps, we introduce new coordinates for the accuracy of numerical calculations,

$$U^{(1)} = \frac{X^{(1)} + X^{(2)}}{2}, \quad U^{(2)} = \frac{Y^{(1)} + Y^{(2)}}{2}, \tag{14a}$$

$$V^{(1)} = \frac{X^{(1)} - X^{(2)}}{2}, \quad V^{(2)} = \frac{Y^{(1)} - Y^{(2)}}{2}. \tag{14b}$$

Then, the coupled Hénon maps of Eq. (13) become

$$U_{t+1}^{(1)} = 1 - a(U_t^{(1)^2} + V_t^{(1)^2}) + 2a\varepsilon(4p-1)U_t^{(1)}V_t^{(1)} - U_t^{(2)}, \tag{15a}$$

$$U_{t+1}^{(2)} = bU_t^{(1)}, \tag{15b}$$

$$V_{t+1}^{(1)} = 2a(\varepsilon - 1)U_t^{(1)}V_t^{(1)} - V_t^{(2)}, \tag{15c}$$

$$V_{t+1}^{(2)} = bV_t^{(1)}. \tag{15d}$$

In this new map, we numerically follow a typical trajectory in the intermittent two-cluster state until its length L becomes 10^8, and obtain its two transverse Lyapunov exponents $\sigma_{\perp,1}$ and $\sigma_{\perp,2}(\leq\sigma_{\perp,1})$ for the trajectory segment.

Figure 5(a) shows the largest transverse Lyapunov exponent $\sigma_{\perp,1}$ which depends on the the asymmetry parameter p [$p=0$ (up triangles), 0.151 (crosses), and 1/3 (down triangles)]. Below a threshold value $p^*(\simeq 0.151)$, the two-cluster is transversely stable (i.e., $\sigma_{\perp,1}<0$), while above p^*, it is transversely unstable (i.e., $\sigma_{\perp,1}>0$). Hence, for $0\leq p<p^*$ partial synchronization occurs through a supercritical blowout bifurcation. On the other hand, complete desynchronization takes place for $p^*<p\leq 1/3$. As in the coupled 1D maps, such a transverse stability of the two-cluster state may be understood through a decomposition of the intermittent two-cluster into its laminar and bursting components. We use a threshold value d^* $(=10^{-4})$ for the transverse variable d $\left[\equiv\frac{1}{2}(|V^{(1)}|+|V^{(2)}|)\right]$, representing the deviation from the invariant synchronization plane. When $d<d^*$, the system is in the laminar (off) state, while for $d\geq d^*$ it is in the bursting (on) state. As in Sec. II A, the sign of the largest transverse Lyapunov exponent $\sigma_{\perp,1}$ of the two-cluster state is determined through the competition between its laminar and bursting components [see Eq. (9b)]. Figures 5(b) and 5(c) show the strength of the laminar and bursting components (i.e., $|\Sigma_{\perp,1}^l|$ and $\Sigma_{\perp,1}^b$), respectively. We note that as p increases from zero [$p=0$ (up triangles), 0.151 (crosses), and 1/3 (down triangles)], $\Sigma_{\perp,1}^b$ increases, while $|\Sigma_{\perp,1}^l|$ is nearly independent of p. For $0\leq p<p^*(\simeq 0.151)$, the laminar component is dominant because $|\Sigma_{\perp,1}^l|>\Sigma_{\perp,1}^b$, and hence a partially synchronized attractor is born through the supercritical blowout bifurcation. On the other hand, for $p^*<p\leq 1/3$, a completely desynchronized 6D attractor appears because the bursting component becomes dominant (i.e., $\Sigma_{\perp,1}^b>|\Sigma_{\perp,1}^l|$).

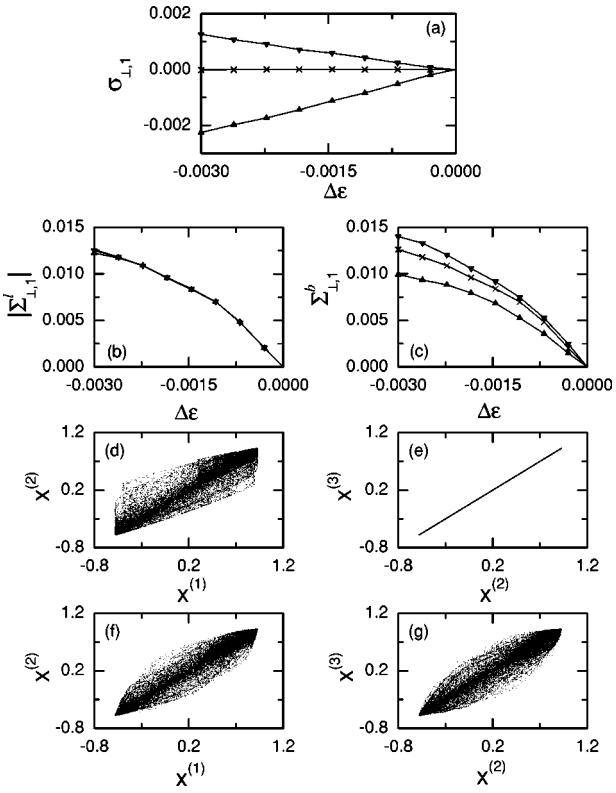

FIG. 5. Consequence of the supercritical blowout bifurcation of the completely synchronized attractor in three coupled Hénon maps for $b=0.1$ and $a=1.83$. (a) Plot of the largest transverse Lyapunov exponent $\sigma_{\perp,1}$ versus $\Delta\varepsilon[\varepsilon-\varepsilon^*(=0.3574)]$ for $p=0$ (up triangles), 0.151 (crosses), and 1/3 (down triangles). (b) [(c)] Plot of the transverse strength of the laminar (bursting) component [i.e., $|\Sigma_{\perp,1}^l|(\Sigma_{\perp,1}^b)$] versus $\Delta\varepsilon$. The symbols are the same as those in (a), and the threshold value for the laminar state is $d^*=10^{-4}$. Straight lines between the data symbols are plotted only to guide the eye. Projections of the partially synchronized attractor onto the (d) $x^{(1)}$-$x^{(2)}$ and (e) $x^{(2)}$-$x^{(3)}$ planes for $\varepsilon=0.34$ in the unidirectionally coupled case with $p=0$. Projections of the completely desynchronized attractor onto the (f) $x^{(1)}$-$x^{(2)}$ and (g) $x^{(2)}$-$x^{(3)}$ planes for $\varepsilon=0.34$ in the symmetrically coupled case with $p=1/3$.

As examples for $\varepsilon=0.34$, see Figs. 5(d), 5(e), 5(f), and 5(g) which show the partially synchronized attractor and the completely desynchronized attractor for $p=0$ and 1/3, respectively.

As a second example, we consider a system of three coupled parametrically forced pendula:

$$\dot{x}_i = y_i + \varepsilon[M_x - x_i], \quad \dot{y}_i = f(x_i, y_i, t) + \varepsilon[M_y - y_i], \tag{16a}$$

$$M_x \equiv (1-2p)x_1 + px_2 + px_3, \quad M_y \equiv (1-2p)y_1 + py_2 + py_3, \tag{16b}$$

where $(x_i y_i)$ $(i=1,2,3)$ is a state vector of the ith pendulum, $f(x,y,t) = -2\pi\beta\Omega y - 2\pi(\Omega^2 - A\cos 2\pi t)\sin 2\pi x$, x is a normalized angle with range $x\in[0,1)$, y is a normalized angular velocity, the overdot denotes a derivative with respect to time t, β is a normalized damping parameter, Ω is a normal-

ized natural frequency of the unforced pendulum, A is a normalized driving amplitude of the vertical oscillation of the suspension point, ε is a coupling parameter, and p ($0 \leqslant p \leqslant 1/3$) is a parameter tuning the degree of the asymmetry in the coupling. The two extreme cases of coupling correspond to the unidirectional ($p=0$) and symmetric ($p=1/3$) couplings, and (M_x, M_y) is a "weighted" mean field. As in the three coupled 1D maps, these three coupled pendula may also be used as a model for studying the three-cluster dynamics in an ensemble of globally coupled pendula.

We fix the values of β, Ω, and A at $\beta=1.0$, $\Omega=0.5$, and $A=0.85$, and investigate the dependence of the occurrence of partial synchronization on the asymmetry parameter p. When the coupling parameter ε decreases and passes a threshold value $\varepsilon^*(=0.648)$, the completely synchronized attractor becomes transversely unstable, independently of p. Then, an asynchronous two-cluster, exhibiting on-off intermittency, appears on an invariant subspace via a supercritical blowout bifurcation. If the two-cluster is transversely stable (unstable), partial synchronization (complete desynchronization) occurs. This two-cluster satisfies $x_1(t) \equiv X_1(t)$, $y_1(t) \equiv Y_1(t)$, $x_2(t)=x_3(t) \equiv X_2(t)$, and $y_2(t)=y_3(t) \equiv Y_2(t)$, and its dynamics is governed by a system of four coupled ordinary differential equations,

$$\dot{X}_1 = Y_1 + 2p\varepsilon[X_2 - X_1], \tag{17a}$$

$$\dot{Y}_1 = f(X_1, Y_1, t) + 2p\varepsilon[Y_2 - Y_1], \tag{17b}$$

$$\dot{X}_2 = Y_2 + (1-2p)\varepsilon[X_1 - X_2], \tag{17c}$$

$$\dot{Y}_2 = f(X_2, Y_2, t) + (1-2p)\varepsilon[Y_1 - Y_2]. \tag{17d}$$

As in the coupled Hénon maps, we introduce new coordinates for the accuracy of numerical calculations,

$$U_1 = \frac{X_1 + X_2}{2}, \quad U_2 = \frac{Y_1 + Y_2}{2}, \tag{18a}$$

$$V_1 = \frac{X_1 - X_2}{2}, \quad V_2 = \frac{Y_1 - Y_2}{2}. \tag{18b}$$

Then, the equations of motion of Eq. (17) become

$$\dot{U}_1 = U_2 + (1-4p)\varepsilon V_1, \tag{19a}$$

$$\dot{U}_2 = -2\pi\beta\Omega U_2 - 2\pi(\Omega^2 - A\cos 2\pi t)\sin 2\pi U_1 \cos 2\pi V_1 + (1-4p)\varepsilon V_2, \tag{19b}$$

$$\dot{V}_1 = V_2 - \varepsilon V_1, \tag{19c}$$

$$\dot{V}_2 = -(2\pi\beta\Omega + \varepsilon)V_2 - 2\pi(\Omega^2 - A\cos 2\pi t) \times \cos 2\pi U_1 \sin 2\pi V_1. \tag{19d}$$

By stroboscopically sampling the orbit points $[U_1(m), U_2(m), V_1(m), V_2(m)]$ at the discrete time m, we obtain the 4D Poincaré map P.

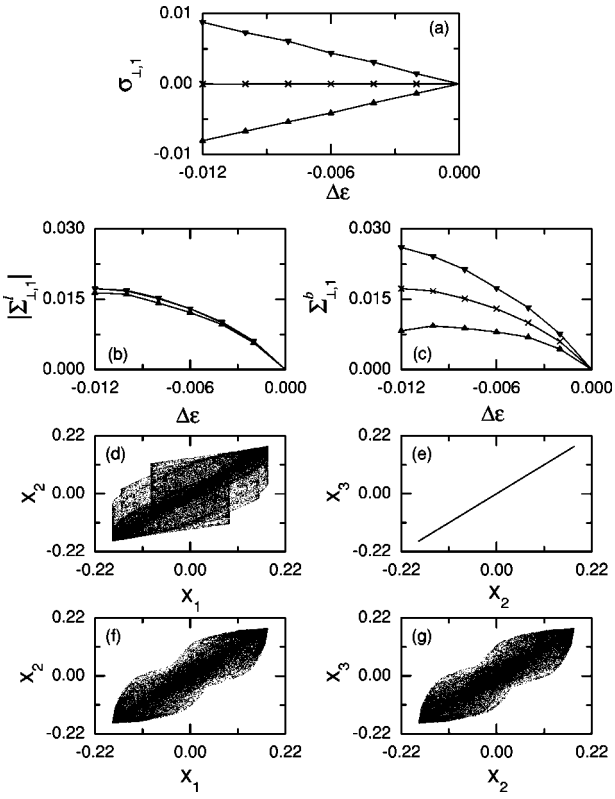

FIG. 6. Consequence of the supercritical blowout bifurcation of the completely synchronized attractor in three coupled pendula for $\beta=1.0$, $\Omega=0.5$ and $A=0.85$. (a) Plot of the largest transverse Lyapunov exponent $\sigma_{\perp,1}$ versus $\Delta\varepsilon[\varepsilon-\varepsilon^*(=0.648)]$ for $p=0$ (up triangles), 0.151 (crosses), and 1/3 (down triangles). (b) [(c)] Plot of the transverse strength of the laminar (bursting) component [i.e., $|\Sigma^l_{\perp,1}|(\Sigma^b_{\perp,1})$] versus $\Delta\varepsilon$. The symbols are the same as those in (a), and the threshold value for the laminar state is $d^*=10^{-4}$. Straight lines between the data symbols are plotted only to guide the eye. Projections of the partially synchronized attractor onto the (d) x_1-x_2 and (e) x_2-x_3 planes for $\varepsilon=0.63$ in the unidirectionally coupled case with $p=0$. Projections of the completely desynchronized attractor onto the (f) x_1-x_2 and (g) x_2-x_3 planes for $\varepsilon=0.63$ in the symmetrically coupled case with $p=1/3$.

As in the coupled Hénon maps, we follow a trajectory in the intermittent two-cluster until its length L becomes 10^8, and obtain its transverse Lyapunov exponents. As shown in Fig. 6(a), the largest transverse Lyapunov exponent $\sigma_{\perp,1}$ depends on p [$p=0$ (up triangles), 0.17 (crosses), and 1/3 (down triangles)]. For $p<p^*(\simeq 0.17)$, the two-cluster is transversely stable with $\sigma_{\perp,1}<0$, while for $p>p^*$, it is transversely unstable with $\sigma_{\perp,1}>0$. Like the cases of the coupled 1D and Hénon maps, this transverse stability of the intermittent two-cluster state (i.e., the sign of $\sigma_{\perp,1}$) may be determined via competition between its laminar and bursting components. The weighted transverse Lyapunov exponents of the laminar and bursting components $|\Sigma^l_{\perp,1}|$ and $\Sigma^b_{\perp,1}$ are shown in Figs. 6(b) and 6(c), respectively. As p is increased from zero [$p=0$ (up triangles), 0.17 (crosses), and 1/3 (down triangles)], the strength of the bursting component (i.e., $\Sigma^b_{\perp,1}$) increases, while the strength of the laminar component (i.e., $|\Sigma^l_{\perp,1}|$) is nearly independent of p. For the threshold value

$p^*(\simeq 0.17)$, the strengths of laminar and bursting components become balanced. Thus, for $0 \leqslant p < p^*$, the two-cluster is transversely stable because the laminar component is dominant, and hence a partially synchronized attractor is created via the supercritical blowout bifurcation [e.g., see Figs. 6(d) and 6(e) for $p=0$ and $\varepsilon=0.63$]. On the other hand, since the bursting component is dominant for $p^* < p \leqslant 1/3$, the two-cluster is transversely unstable, and hence a completely desynchronized attractor appears [e.g., see Figs. 6(f) and 6(g) for $p=1/3$ and $\varepsilon=0.63$].

III. SUMMARY

We have investigated the dynamical origin for the appearance of a partially synchronized attractor via a blowout bifurcation of the fully synchronized attractor in three coupled 1D (noninvertible) maps. An asynchronous two-cluster state appears on an invariant plane through the supercritical blowout bifurcation, and it exhibits on-off intermittency. It has been found that the transverse stability of the intermittent two-cluster state may be determined via competition between its laminar and bursting components. If the laminar component is dominant, then partial synchronization occurs on the invariant plane; otherwise complete desynchronization takes place. These results are also confirmed in three coupled Hénon maps and three coupled pendula which are multidimensional invertible period-doubling systems. Hence, the mechanism for the occurrence of partial synchronization seems to be "universal," in the sense that it holds in typical three-coupled period-doubling systems.

ACKNOWLEDGMENT

This work was supported by the Korea Science and Engineering Foundation (Grant No. R05-2004-000-10717-0).

[1] K. M. Cuomo and A. V. Oppenheim, Phys. Rev. Lett. **71**, 65 (1993); L. Kocarev, K. S. Halle, K. Eckert, L. O. Chua, and U. Parlitz, Int. J. Bifurcation Chaos Appl. Sci. Eng. **2**, 973 (1992); L. Kocarev and U. Parlitz, Phys. Rev. Lett. **74**, 5028 (1995); N. F. Rulkov, Chaos **6**, 262 (1996).
[2] H. Fujisaka and T. Yamada, Prog. Theor. Phys. **69**, 32 (1983).
[3] A. S. Pikovsky, Z. Phys. B: Condens. Matter **50**, 149 (1984).
[4] V. S. Afraimovich, N. N. Verichev, and M. I. Rabinovich, Radiophys. Quantum Electron. **29**, 795 (1986).
[5] L. M. Pecora and T. L. Carroll, Phys. Rev. Lett. **64**, 821 (1990).
[6] E. Ott and J. C. Sommerer. Phys. Lett. A **188**, 39 (1994).
[7] P. Ashwin, P. J. Aston, and M. Nicol, Physica D **111**, 81 (1998).
[8] Y. Nagai and Y.-C. Lai, Phys. Rev. E **55**, R1251 (1997); **56**, 4031 (1997).
[9] P. Glendinning, Phys. Lett. A **264**, 303 (1999).
[10] S.-Y. Kim, W. Lim, E. Ott, and B. Hunt, Phys. Rev. E **68**, 066203 (2003).
[11] K. Pyragas, Phys. Rev. E **54**, R4508 (1996).
[12] M. S. Vieira and A. J. Lichtenberg, Phys. Rev. E **56**, R3741 (1997).
[13] M. Hasler, Yu. Maistrenko, and O. Popovych, Phys. Rev. E **58**, 6843 (1998); Yu Maistrenko, O. Popovych, and M. Hasler, Int. J. Bifurcation Chaos Appl. Sci. Eng. **10**, 179 (2000); A. V. Taborov, Yu. Maistrenko, and E. Mosekilde, *ibid.* **10**, 1051 (2000); S. Yanchuk, Yu. Maistrenko, and E. Mosekilde, Chaos **13**, 388 (2003).
[14] M. Inoue, T. Kawazoe, Y. Nishi, and M. Nagadome, Phys. Lett. A **249**, 69 (1998).
[15] Y. Zing, G. Hu, H. A. Cerdera, S. Chen, T. Braun, and Y. Yao, Phys. Rev. E **63**, 026211 (2001).
[16] N. Tsukamoto, S. Miyazaki, and H. Fujisaka, Phys. Rev. E **67**, 016212 (2003).
[17] K. Kaneko, Physica D **41**, 137 (1990).
[18] O. Popovych, Yu. Maistrenko, and E. Mosekilde, Phys. Rev. E **64**, 026205 (2001).
[19] O. Popovych, Yu. Maistrenko, and E. Mosekilde, Phys. Lett. A **302**, 171 (2002).
[20] A. S. Pikovsky and P. Grassberger, J. Phys. A **24**, 4587 (1991); A. S. Pikovsky, Phys. Lett. A **165**, 33 (1992).
[21] H. Fujisaka and T. Yamada, Prog. Theor. Phys. **74**, 918 (1985); **75**, 1087 (1986); H. Fujisaka, H. Ishii, M. Inoue, and T. Yamada, *ibid.* **76**, 1198 (1986).
[22] L. Yu, E. Ott, and Q. Chen, Phys. Rev. Lett. **65**, 2935 (1990); Physica D **53**, 102 (1992).
[23] N. Platt, E. A. Spiegel, and C. Tresser, Phys. Rev. Lett. **70**, 279 (1993); J. F. Heagy, N. Platt, and S. M. Hammel, Phys. Rev. E **49**, 1140 (1994); N. Platt, S. M. Hammel, and J. F. Heagy, Phys. Rev. Lett. **72**, 3498 (1994).
[24] S. C. Venkataramani, T. M. Antonsen, E. Ott, and J. C. Sommerer, Physica D **96**, 66 (1996).
[25] M. Ding and W. Yang, Phys. Rev. E **56**, 4009 (1997).
[26] H. L. Yang and E. J. Ding, Phys. Rev. E **50**, R3295 (1994).
[27] A. Čenys and H. Lustfeld, J. Phys. A **29**, 11 (1996).
[28] D. Marthaler, D. Armbruster, Y.-C. Lai, and E. Kostelich, Phys. Rev. E **64**, 016220 (2001).
[29] When the magnitude of a transverse variable d of a typical trajectory in the two-cluster state, representing the deviation from the invariant synchronization line, is less than a threshold value $\tilde{d}$, the computed trajectory falls into an exactly synchronous state due to the finite precision. In the system of coordinates X and Y, the order of magnitude of the threshold value $\tilde{d}$ for $d(=|X-Y|)$ is about 10^{-15} except in the region near the origin, because the double-precision values of X and Y have about 15 decimal places of precision. On the other hand, in the system of U and V, the order of magnitude of the threshold value $\tilde{d}$ for d $(=|V|)$ is about 10^{-308}, which is a threshold value for numerical underflow in the IEEE (Institute of Electrical and Electronics Engineers) double-precision calculation. Hence, in the system of U and V, we can follow a trajectory until its length becomes sufficiently long for the calculation of Lyapunov exponents of the two-cluster state.
[30] The weighted transverse Lyapunov exponents $\Sigma_\perp^l$ and $\Sigma_\perp^b$ of

the laminar and bursting components depend on the threshold value d^* for the laminar state, while the transverse Lyapunov exponent $\sigma_\perp$ of the two-cluster state is independent of d^*. As d^* is decreased, $\Sigma_\perp^l$ decreases to zero because the fraction μ_l of the time spent in the laminar state goes to zero; thus $\Sigma_\perp^b$ $[=\sigma_\perp+|\Sigma_\perp^l|]$ converges to $\sigma_\perp$. However, we note that $\sigma_\perp$ depends only on the difference between $\Sigma_\perp^b$ and $|\Sigma_\perp^l|$, which is independent of d^* [see Eq. (9b)]. Hence, although $\Sigma_\perp^{l(b)}$ depends on d^*, the conclusion as to the transverse stability of the the two-cluster state is independent of d^*.